Earthquake Engineering, Tenth World Conference © 1992 Balkema, Rotterdam. ISBN 90 5410 060 5

Dynamic response of H-shaped steel beam-columns under two-directional ground motion

Yasuhiro Uchida
Kagoshima University, Japan
Shosuke Morino, Jun Kawaguchi & Takeshi Koyama
Mie University, Japan

ABSTRACT: This paper first presents the results of shaking table tests of steel cantilever beam-columns with H-shaped section subjected to uniaxial or biaxial bending by the ground motion of the sinusoidal wave, with the results of the dynamic analysis. Then discussed is the dynamic response behavior of steel beam-columns failing in the local buckling and/or in the increase of out-of-plane displacement, focusing the effects of experimental parameters; width-to-thickness ratio, direction and frequency of the ground motion, and amount of mass eccentricity. In general, the lateral instability behavior observed in the shaking table tests seems more drastic than that observed in the static monotonic loading tests, and then the present design provisions may need be amended.

1 INTRODUCTION

The structural behavior of a building frame is independently investigated in two orthogonal directions in many cases of the structural design, although both the structure itself and the input earthquake motion possess the three-dimensional characteristics, since the three-dimensional dynamic behavior of members and structures is not yet well clarified, and the method for the safety evaluation is not established.

The paper first introduces the results of the shaking table tests of steel beam-columns with H-shaped section subjected to one- or two-directional ground motion of the sinusoidal wave, with the results of the dynamic analysis. Then discussed is the elasto-plastic dynamic response behavior of steel beam-columns failing in the local buckling and/or in the increase of the out-of-plane displacements, focusing the effects of the direction and the frequency of the ground motion, the mass eccentricity and the width-to-thickness ratio of plate elements.

2 SHAKING TABLE TESTS OF CANTILEVER BEAM-COLUMNS

2.1 Specimen

The specimen of the shaking table test is a cantilever beam-column subjected to the constant axial force by the weight at the top. Experimental parameters selected are as follows: width-to-thickness ratio b/t; direction of the ground motion θ; frequency of the ground motion f_g; and amount of mass eccentricity ratio $\bar{e}$. Measured dimensions and cross-sectional properties are listed in Table 1. Two letters at the top of the specimen's name indicate the width-to-thickness ratio: WH stands for an H-section with b/t=15, and NH for an H-section with b/t=7. In addition, the specimen's name consists of the sequential number and a letter indicating the bending or torsional conditions: U for the specimen subjected to uniaxial bending; B for biaxial bending; and E for torsion with the mass eccentricity. Specimens are built-up from SS400 steel plates by welding and annealed to remove resisual stresses. The yield stress of the steel plate is 320kN/mm^2, the tensile strength 414kN/mm^2 and the elongation 25.9%. Young's modulus E is 2058 MN/mm^2.

Table 2 shows natural frequency f_o and damping ratio h obtained from the free vibration test, together with the computed natural frequency f_o', where x- and y-axes are the strong and weak axes of H-section, respectively. Experimental values for the natural frequency are a little smaller than the computed values, because of the imperfect base fixity and the restraint of the measuring devices. The values of damping ratio are different in two directions.

2.2 Loading condition

Table 3 shows the loading condition. The value of θ indicates the angle between the shaking axis of the table Y and the weak axis

of H-section y, as shown in Fig. 2. The direction of the ground motion for 3B and 4B specimens of WH and NH series makes an angle of about 18° to y-axis, which is determined so that the ratio of the input forces in two directions is nearly equal to the ratio of the yield shear forces in two directions. These specimens are thus subjected to biaxial bending. The frequency of the ground motion f_g is set equal to the nominal value of the natural frequency in y-direction for 1U, 3B, 5E and 6E specimens of WH and NH series, whereas f_g is set equal to the natural frequency computed in x-direction for 2U and 4B specimens of WH and NH series. The mass eccentricity ratio $\bar{e}$ is defined as follows:

$$\bar{e} = e/\sqrt{K_\theta/K_y} \quad (1)$$

where e is the distance between the center of the mass(=center of gravity) and the center of the cross section; K_θ is the torsional rigidity; and K_y is the horizontal sway rigidity in y-axis. The ratio of the applied axial force to the yield axial force P/P_y is from 0.013 to 0.016.

In the test, the weight is first applied on the specimen. Then, the table starts shaking with the sinusoidal wave of the acceleration with a low amplitude, and the acceleration amplitude is increased in a stepwise manner by the manual operation, until the specimen collapses. Therefore, the time-history record of the ground motion is different for each specimen.

Table 1 Dimensions and cross-sectional properties of specimens

name	WH1U	WH2U	WH3B	WH4B	WH5E	WH6E	NH1U	NH2U	NH3B	NH4B	NH5E	NH6E
L(cm)	149.9	149.6	149.6	149.7	149.8	149.8	99.7	99.8	99.7	99.7	99.8	99.8
B(cm)	6.93	6.94	6.94	6.94	6.94	6.94	3.35	3.34	3.35	3.35	3.34	3.34
H(cm)	7.37	7.40	7.41	7.42	7.49	7.36	3.79	3.80	3.80	3.79	3.77	3.80
t_w(cm)	0.23	0.23	0.22	0.23	0.22	0.23	0.23	0.22	0.22	0.23	0.22	0.23
t_f(cm)	0.23	0.23	0.24	0.24	0.23	0.24	0.23	0.23	0.24	0.23	0.24	0.24
A(cm^2)	4.79	4.77	4.76	4.94	4.80	4.89	2.33	2.30	2.33	2.31	2.30	2.34
w/t_w	30	30	32	30	32	30	15	15	15	15	15	15
$B/2t_f$	15	15	15	14	15	15	7	7	7	7	7	7
λ x	103	102	101	102	101	103	138	138	137	138	139	138
y	197	197	194	195	196	196	271	272	269	272	270	271

Note: L = length of specimen, B = width of section, H = hight of section, t_f = thickness of flange, t_w = thickness of web, A = sectional area, $B/2t_f$ = width-thickness ratio of flange, w/t_w = width-thickness ratio of web, and λ = slenderness ratio

Table 2 Dynamic characteristics of specimens

name		WH1U	WH2U	WH3B	WH4B	WH5E	WH6E	NH1U	NH2U	NH3B	NH4B	NH5E	NH6E
f_o(Hz)	x	1.29	1.28	1.29	1.30	1.33	1.31	1.14	1.13	1.13	1.13	1.13	1.12
	y	2.50	2.45	2.50	2.54	2.50	2.51	2.41	2.42	2.43	2.41	2.41	2.39
f_o'(Hz)	x	1.49	1.49	1.51	1.53	1.47	1.48	1.27	1.27	1.29	1.27	1.21	1.22
	y	2.86	2.87	2.89	2.94	2.85	2.82	2.50	2.50	2.52	2.49	2.37	2.41
h(%)	x	1.43	1.77	1.65	1.72	0.90	0.71	1.77	1.54	1.50	1.38	1.22	1.38
	y	1.19	1.25	1.27	1.76	0.97	0.82	1.43	0.81	0.76	0.80	0.69	0.74

Note: f_o = natural frequency (experiment), f_o' = natural frequency (calculated), and h = damping ratio (experiment)

Table 3 Loadig condition

name	WH1U	WH2U	WH3B	WH4B	WH5E	WH6E	NH1U	NH2U	NH3B	NH4B	NH5E	NH6E
θ(°)	0	0	18	18	0	0	0	0	18	18	0	0
f_g(Hz)	2.5	1.3	2.5	1.3	2.5	2.5	2.4	1.1	2.4	1.1	2.4	2.4
$\bar{e}$(%)	0	0	0	0	10	20	0	0	0	0	10	20
P/P_y	0.014	0.014	0.014	0.013	0.014	0.014	0.015	0.015	0.015	0.015	0.016	0.016

Note: θ = shaking direction, f_g = input frequency, $\bar{e}$ = mass eccentricity ratio, and P/P_y = ratio of axial force to ultimate axial thrust

2.3 Test set-up

The test set-up on the shaking table is shown in Fig. 1. Several steel plates as the weights are fixed by bolts on the top plate of the specimen. The measuring system is shown in Fig. 2 schematically, where the horizontal displacements in the shaking direction (Y-direction) and its perpendicular direction (X-direction), and the twisting angle of the top plate of the specimen are measured by 3 displacement meters. The acceleration at the top plate in X- and Y-directions, and the acceleration of the table in Y-direction are measured by the acceleration meters. The longitudinal strains of the specimen at the point 30mm apart from the base are measured by the wire strain gauges to grasp the initiation of the local buckling.

3 DYNAMIC RESPONSE ANALYSIS

3.1 Model for the analysis

A cantilever model of length ℓ is adopted for the dynamic analysis as shown in Fig. 3. In order to simplify the computational task, assumptions are made as follows:

1. The deformable portion is concentrated at the column base with length $d\ell$, in which the cross-sectional plane remains the plane after the deformation occurs. Other portion is rigid.
2. The stress σ and the strain ε in the deformable portion obey the bilinear type relation shown in Fig. 4, where σ_y = yield stress, ε_y = yield strain.
3. Biaxial curvatures are uniformly distributed along the deformable portion of length $d\ell$. Thus, the displacements u and v at the top of the cantilever in x- and y-directions, respectively, are given as follows:

$$u = \phi_y \cdot d\ell \cdot \ell, \quad v = \phi_x \cdot d\ell \cdot \ell \qquad (2)$$

where ϕ_x, ϕ_y = curvatures about x- and y-axes, respectively.

4. Only deformations due to biaxial bending are considered. Axial elongation, torsional deformation and shear deformation are all neglected.
5. Initial imperfections such as resisual stress and initial curvature are not considered. The local buckling does not occur.

Once the biaxial bending moment-curvature relation is calculated from the stress-strain curve shown in Fig. 3, the relation between the shear force working on the cantilever and the top displacement is calculated by the iterative procedure from Eq. (2) and the equilibrium equations in two directions, i.e.,

$$Q_x = (M_y - P \cdot u)/\ell, \quad Q_y = (M_x - P \cdot v)/\ell \qquad (3)$$

where Q_x, Q_y = shear forces, and M_x, M_y = bending moments at the base about x- and y-axes, respectively.

3.2 Equations of motion of one-mass system

The equations of motion of one-mass system shown in Fig. 3 are written in a dimensionless form as follows:

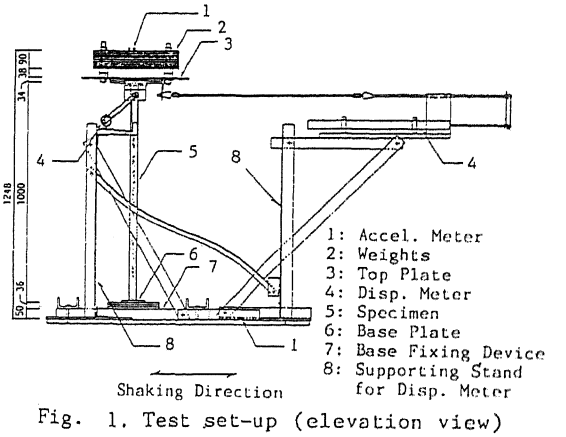

Fig. 1. Test set-up (elevation view)

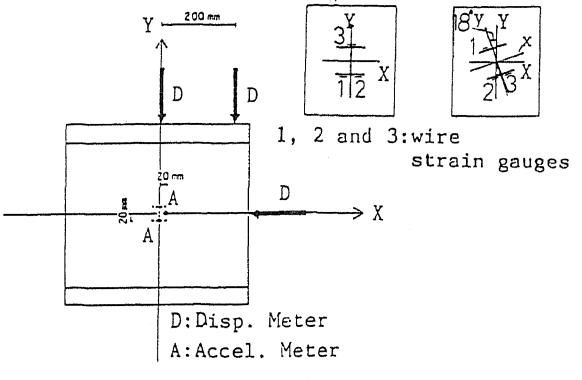

Fig. 2. Set of measuring devices

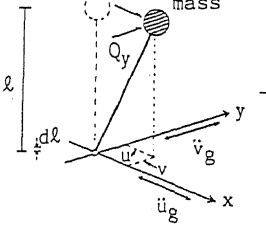

Fig. 3. Model for analysis

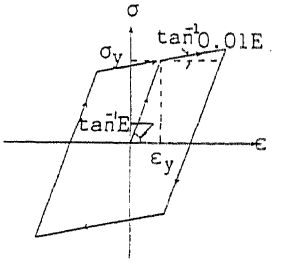

Fig. 4. Stress-strain relation

$$\ddot{u}/u_o+2h_x\cdot\omega_x\cdot\dot{u}/u_o+\omega_x^2\cdot Q_x/Q_{xo}=-\omega_x^2\cdot\ddot{u}_g/(Q_{xo}/M) \quad (4)$$

$$\ddot{v}/v_o+2h_y\cdot\omega_y\cdot\dot{v}/v_o+\omega_y^2\cdot Q_y/Q_{yo}=-\omega_y^2\cdot\ddot{v}_g/(Q_{yo}/M)$$

where ω = natural frequency of the elastic cantilever($=\sqrt{k/M}$), k = elastic stiffness, M = mass, C = critical damping coefficient, h = damping ratio($= C/\sqrt{k\cdot M}/2$); ($\cdot$) indicates the derivative with respect to the time, x and y the quantities corresponding to x- and y-axes, respectively, o the value at the initial yielding at the base, and g the value with respect to the ground.

Iterative procedure taken in the numerical computation to solve the equation of motion is Newmark's β method, where β is taken equal to 1/4. As to the computational details, the readers should refer to Ref. [1].

4. TEST RESULTS AND DISCUSSION

Figure 5 shows time-history records of the ground motion, displacements in two directions and strain of NH1U, together with the relation between the response acceleration and displacement, and displacement path. The center of time-history curve of the displacement u in (c) starts to drift away with the occurrence of the local buckling which is recognized by the drift of strain in (d). The strength in y-direction in (e) reaches the strength given by the rigid plastic collapse mechanism line indicated by broken line, in spite of the local buckling. This specimen is subjected to uniaxial bending, but it finally collapses due to the lateral instability with the displacement u accumulating excessively. This phenomenon is clearly observed in the results of both test and analysis. In the analysis, the input ground acceleration with the amplitude of $Q_{xo}/M/1000$ is given in x-direction, and the specimen is treated as subjected to biaxial bending. This treatment well traces the displacement accumulation as observed in (g) and (h). Plastification of the cross section and the local buckling may have caused the displacement accumulation beyond the limit of convergence, and the out-of-plane displacement increases with the increase of the repetition cycle. The increase of out-of-plane displacement may also have occurred due to the divergent vibration of the beam-column with the instantaneous strength deterioration in y-direction caused by PΔ effect and plastification of the flanges. Details of the convergence-divergence phenomenon with the displacement accumulation are explained in Ref. [2].

Figure 6 shows the results of the specimen NH3B to which the ground motion is applied in the direction with an angle of 18° to the principal axis y of the cross section. Because of the interaction between biaxial bending moments, the strength in y-direction gradually deteriorates as observed in (a), whereas the strength in x-direction in (c) becomes larger. It seems that the displacement in x-direction of the specimen under two-directional shaking increases more slowly than that under the one-directional shaking. The energy absorption capacity of the specimen under two-direction shaking is found to be greater than that under the y-directional shaking, such as NH1U.

Figure 7 shows the results of the specimen WH3B. Loading condition of the specimen WH3B is almost the same as that of NH3B, but is likely to be more affected by the local buckling because of the greater width-thickness ratio. The out-of-plane displacement increases rather gradually compared with NH3B, due to the change of the dynamic characteristics caused by the local buckling.

Figure 8 shows the results of the specimen NH4B. For this specimen and WH4B, the frequency of the ground motion is set equal to the natural frequency of the specimen in x-direction in order to observe the resonance phenomenon in x-direction. The amplitudes of the acceleration input to these specimens are in fact larger than those to other specimens, but the specimens are only partially yielded, and the collapse does not occur. The displacement path shows an ellipse-like shape, indicating no specific dominating direction of the displacements, because of the phase difference between the ground acceleration and the response acceleration.

Figure 9 shows the results of the specimen WH6E. This specimen with the mass eccentricity ratio of 20 % is tested to investigate the torsional behavior, together with WH5E, NH5E and NH6E. Sharp reduction of the strength appears in (a) due to the local buckling. However, the torsional angle stays within a small value which is not shown here. From the tests of other specimens with the mass eccentricity, it is observed that the strength deteriorates more rapidly and the displacement u accumulates more with the increase of the mass eccentricity, but the rate of the accumulation of displacement u is not greater than that under one-directional shaking with no eccentricity.

5. CONCLUDING REMARKS

The following results are observed in the shaking table tests and the analysis.

1. All specimens collapse due to the weak-axis bending with the excessive displacement u. Even though the specimen is subjected to the uniaxial ground motion, the failure mode is the lateral instability, which may be caused by the displacement accumulation beyond the limit of convergence.
2. In the specimens subjected to the ground motion with the frequency equal to the natural frequency in x-direction, the dis-

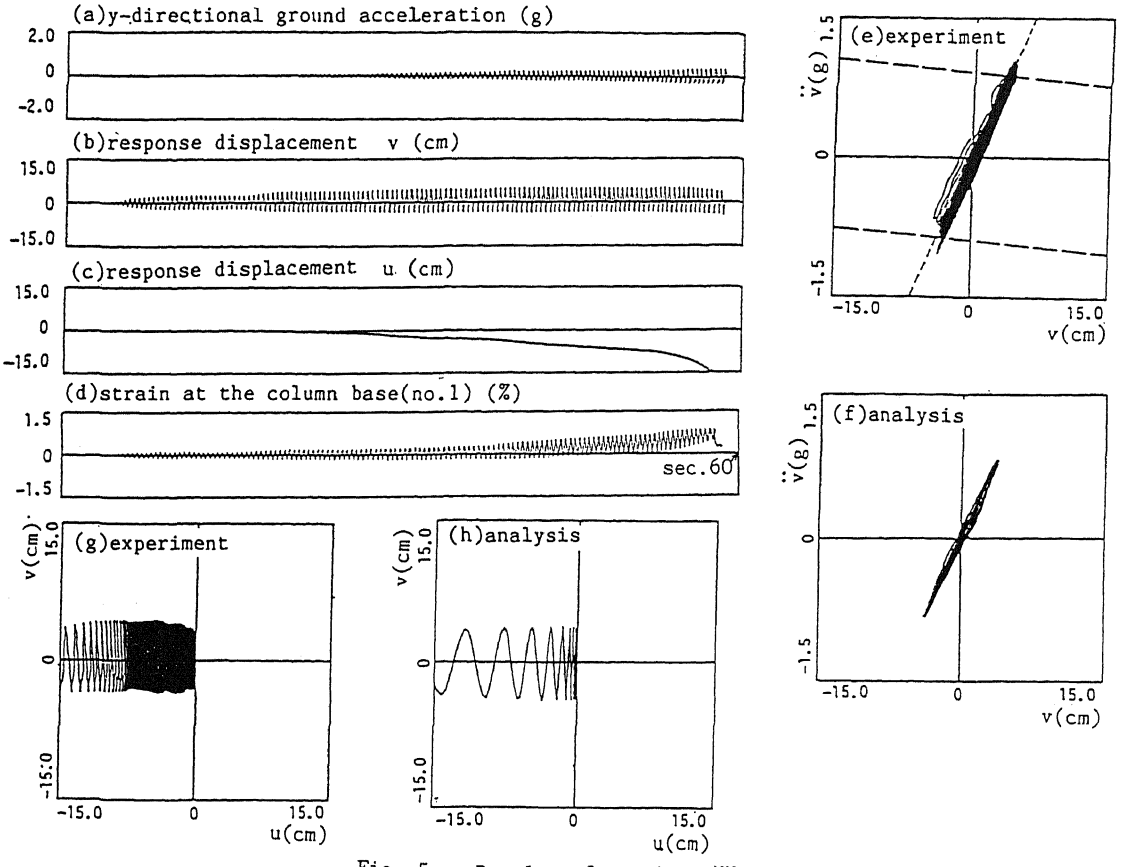

Fig. 5.. Results of specimen NH1U

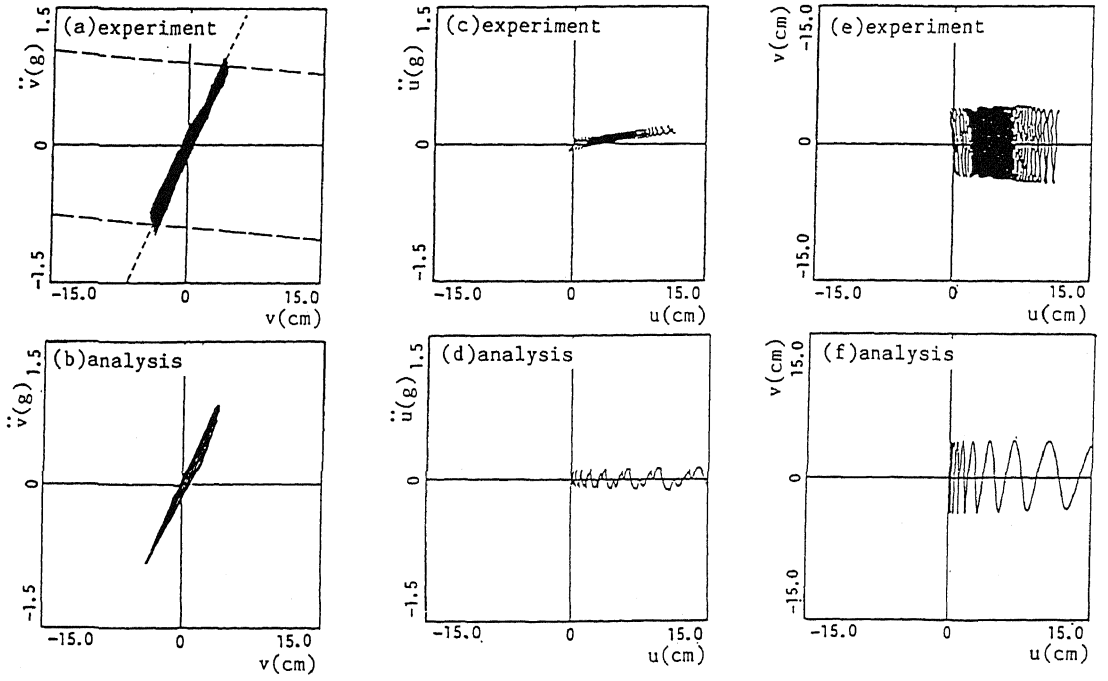

Fig. 6. Results of specimen NH3B

placement path shows an ellipse-like shape without any dominating direction of the displacement, and the torsional vibration sometimes appear.
3. The rate of the strength deterioration is severer in WH series specimens with the larger width-thickness ratio than in NH series specimens, but overall behaviors are quite similar in both series.
4. The increase in the mass eccentricity causes reduction of the maximum strength, severer strength deterioration, and greater out-of-plane deformation.

Acknowledgment This research was funded by a Grant-in-Aid of Scientific Research of Ministry of Education, Japan(1985-1987). The authors wish to express sincere gratitude to the former students, Messrs. Yukitoshi Yoshimura, Hiroshi Iuchi, Katsuya Shimanaka and Takeshi Kunii for their help.

REFERENCES

[1] Morino, S. & Y. Uchida 1980. Dynamic response of steel space frames under earthquake excitation in horizontal arbitrary direction, Proc. of 7WCEE, Vol. 5: 439-442.
[2] Uchida, Y. & S. Morino 1988. Seismic resistance capacity of degrading beam-columns under biaxial bending, Proc. of 9WCEE, Vol.4: 145-150.

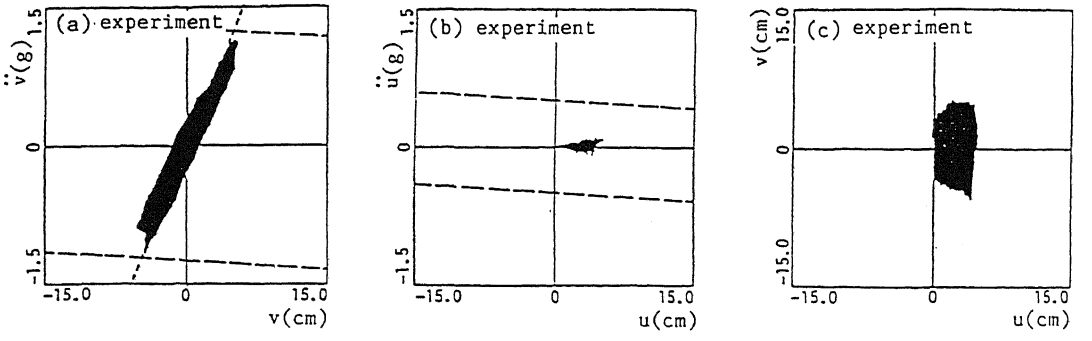

Fig. 7. Results of specimen WH3B

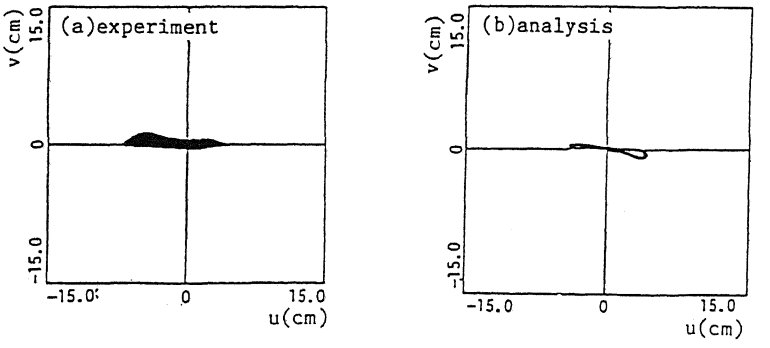

Fig. 8. Results of specimen NH4B

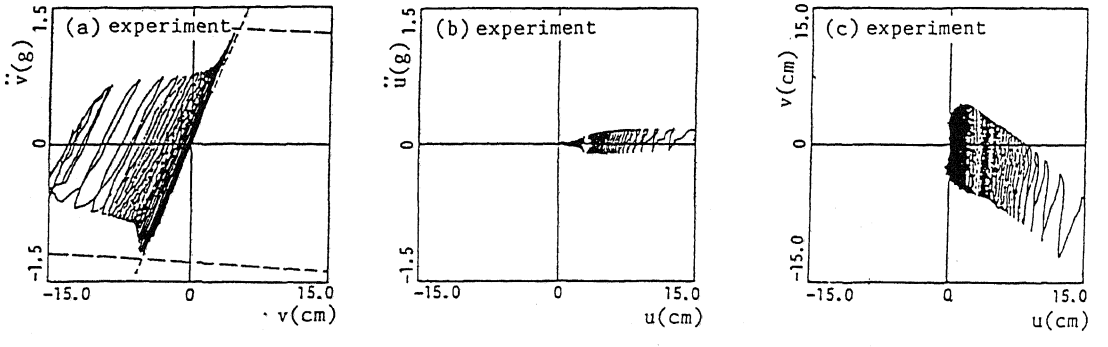

Fig. 9. Results of specimen WH6E